Single-sensor acquisition without data jitter: a comparative sensor study

Nicolas Tellier[1*], Stéphane Laroche[1], Han Wang[1] and Philippe Herrmann[1] present data-supported comparisons between two sensors and discuss their impact on final imaging.

Introduction

Seismic sensors are key components of the acquisition chain. Geophones have been used since the early days of seismic acquisition. Although still based on a moving coil detector, there have been improvements over time, such as higher sensitivities, lower resonant frequencies or rare-earth magnet technologies. The way they are used has, however, evolved. Arrays of several dozen geophones now belong to the past, as operators now favour higher-trace densities with reduced arrays or single sensors. In the early 2000s, a competitor started challenging the geophone monopoly. MEMS (Micro Electro Mechanical Systems) receivers began to replace the last analogue component in the acquisition chain, whereas recording systems had made the leap more than 20 years previously. Their introduction was, however, ahead of its time, as the industry was not ready to replace large geophone arrays with denser (and hence more expensive) spreads. Later on, in the early 2010s, the trend for broadband did not favour MEMS technology either, as the sensors available at that time showed an increase in noise floor towards the low frequency that could compromise the recording of the lowest frequencies.

However, in the 2020s, we are a long way on from the 2000s. The benefits of dense, single-sensor acquisitions are now well recognized by major names in our industry. Whereas high-trace densities have proven to make a significant contribution to processing in order to produce clearer images and more detailed reservoir characterization, the weak signal associated with single-source, single-sensor acquisition is becoming the input data for processing. Although the shortcomings of geophones smooth out when used in large arrays, these shortcomings become an input data artefact for processing when the geophones are used as single sensors. Meanwhile, the third, latest generation of MEMS sensors have, among other improvements, overcome the low-frequency limitation associated with previous generations.

After further investigations into sensor performance, it has been possible to identify several shortcomings inherent in geophones, and their impact on the data acquired that exhibit a clear sensor-related jitter. After a short reminder about sensor technologies, this paper presents data-supported comparisons between the two sensors and discusses their impact on final imaging. These conclusions are sufficiently compelling to convince the leading seismic equipment manufacturer to switch to MEMS for all its new products.

Geophones and MEMS fundamentals

Technology overview

Geophones and MEMS sensors both perform as they are supposed to, i.e., by measuring ground particle motion, using the same principle: a mass-spring device. Apart from being mounted inside a casing, the common points end there! A few purely hardware differences are worth noting:

- MEMS are digital sensors. Geophones are pure analogue ones.
- Their difference in size therefore more or less follows the same logic as the difference between an audio tape and a compact disc: 8 to 20 g for the proof mass of a geophone, versus… only 50 mg for that of a MEMS sensor.
- For geophones, the {spring stiffness/mass weight} ratio is low. For MEMS sensors, it is the opposite.
- As a result, geophones have a low resonant frequency (typically ranging from 5 to 10 Hz, and much lower for some long-period detectors used for academic purposes). MEMS sensors have a much higher resonant frequency (> 800 Hz), and even no resonant frequency when operated in a closed loop.

The first consideration may require some exegesis (Figure 1). Geophones are pure analogue devices since their sensing principle relies on an induced voltage, generated by a coil (attached to the casing through a spring, and thus acting as a proof mass) moving relatively to a magnet (attached to the sensor spike). While MEMS sensors operate upon the same mass-spring principle, the way they sense signal is completely different. With closed-loop MEMS sensors, we do not want the (light) proof mass to move. Instead, to counteract the inertial force on the mass due to ground acceleration, an electrostatic feedback force is applied to the mass by an electronic ASIC (Application Specific Integrated Circuit) switching a voltage signal on its electrodes to keep the proof mass still. As a result, an exact measurement of ground acceleration is provided by an accurate monitoring of this voltage owing to the high-performance associated with the electronic ASIC: the acceleration measurement is then digital.

Further considerations about MEMS technology and how it compares to geophones have been made e.g. by Lainé (2014) and Tellier (2017).

[1] Sercel
[*] Corresponding author, E-mail: nicolas.tellier@sercel.com
DOI: xxx

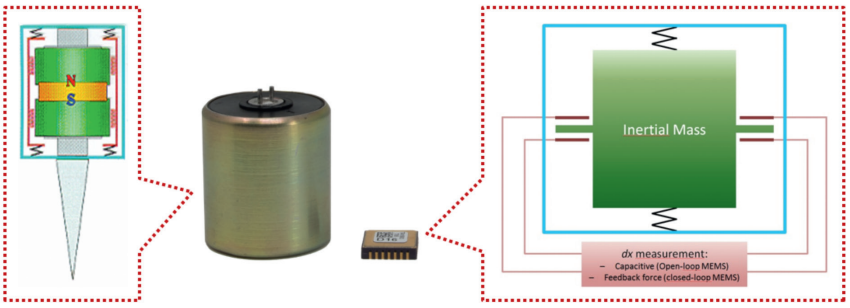

Figure 1 Comparison of geophone and MEMS technologies. Despite marked differences in weight, size, measurement principle and performance, both sensors still rely on the same principle for signal sensing: a mass-spring device.

Sensor output and processing

The output of a geophone is the voltage induced by the magnet displacement within the coil. This voltage is proportional to the ground velocity above the geophone's natural frequency: the conversion into m/s then requires application of the geophone's sensitivity, provided by manufacturers with tolerances. Around and below its natural frequency, the geophone response is no longer linear: besides sensitivity, damping and natural frequency (also provided with tolerances) have to be taken into account to design a second-order operator that can be used to remove the sensor signature.

As a digital sensor, MEMS output is a 24-bit digital signal (signal encrypted on 23 bits, plus one bit for sign), that reflects the force applied to the proof mass to keep it still. This force, and then the sensor output, is proportional to the ground acceleration. By design, it is also flat on the entire seismic bandwidth of interest, from DC (0 Hz). A unique scalar then has to be applied to convert the MEMS digital output into an acceleration, whatever the frequencies involved. Obtaining a ground velocity or ground displacement (increasingly considered for full-waveform inversion) requires the application of a single or double integration. This simple process is supported by most processing software. As it is equipment-independent (flat answer and minor tolerance on MEMS gain), it proves to be much more robust than the geophone designature, and allows a perfect conversion into the physical units of interest. Further considerations relating to uncertainties when converting sensor output into physical units of interest are discussed in the 'Data Jitter' section below.

Third-generation MEMS sensors

The literature abounds with examples of successful deployments of MEMS sensors for mining (e.g., Meisheng et al., 2008), 3C applications (e.g., Stotter, 2011), thin gas reservoir identification from preserved far-offset AVO (e.g., Shi et al., 2008 and 2009), or tight oil exploration (Xuming et al., 2014). MEMS sensors have also widely been used for hydrocarbon applications in regions such as China or North and South America.

The first two generations of MEMS sensors did however encounter difficulties in supporting industry expectations for low-frequency signals, which started about ten years ago. Their noise floor does increase towards the low-frequency (~120 ng/√Hz @ [1-10 Hz] bandwidth for MEMS specified at 40-45 ng /√Hz @ [10-200 Hz] bandwidth), and can prevent the recording of weak signals below a few hertz. This issue has been resolved with the 3rd generation of MEMS (30 ng/√Hz @ [1-10 Hz] and 15 ng /√Hz @ [10-200 Hz]), and the excellent low-frequency performances of the sensor demonstrated (Fougerat 2018, Tellier 2020).

In addition to this low-frequency limitation, MEMS sensors also used to be benchmarked with geophone arrays, which makes the single-sensor solution more costly (more channels required). This is, however, not the case when comparing single MEMS channels to single geophones connected to digitizers. Industrialization efforts have moreover made it possible to reduce the MEMS technology cost even further, now making a MEMS-based channel solution slightly cheaper than its geophone counterpart. The power consumption of the 3rd generation has also been divided by two compared to the previous generation. As an example, for a cabled system, this translates into less field units between digital channels than analogue channels, hence less batteries and less logistics.

To further illustrate the geophysical differences between MEMS sensors and geophones, it is necessary to consider sensing artefacts, which are the biases introduced into the recorded signal by the sensors themselves. In this regard, two sensor-related artefacts are distinguished and discussed in the following sections: signal recording-induced noise and data jitter.

Signal recording-induced noise

Definition

Signal recording-induced noise is the noise associated with the recording of seismic signal. This noise does not affect the seismic signal: it is additional noise, directly related to signal sensing. In addition to sensor distortion that is significantly greater for geophones (-62 dB) than for MEMS sensors (-90 dB), two types of signal recording-induced noise have already been identified.

Electro-magnetic contamination

As the principle of geophone sensing is based on a coil-magnet device, this makes this sensor particularly sensitive to environmental electromagnetic noise. Although sources of electromagnetic noise are numerous, particularly in urban areas, power lines constitute the main contributor. Now present on most surveys, their 50/60 Hz signal and associated harmonics produce an induced voltage on the geophone coil-magnet sensing element that is recorded on the seismic tape. This noise is even stronger when a non-balanced geophone array is used. Contrary to the case with geophones, MEMS records are inherently free from this contamination, as the sensing is not based on a coil-magnet detector.

This phenomenon is well-known by geophysicists and examples are numerous. Figure 2 provides an additional illustration

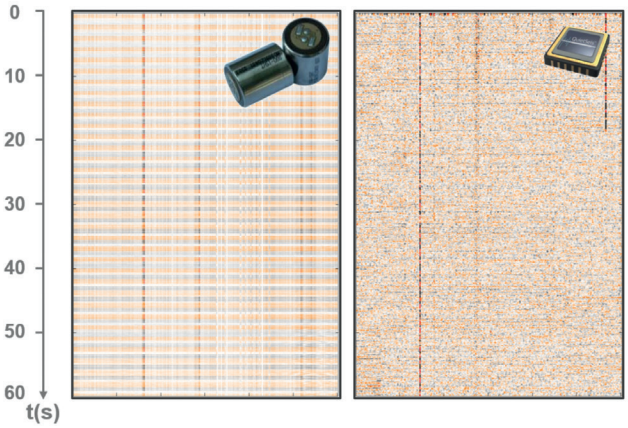

Figure 2 A 60-second passive record acquired by a 10 Hz geophone (left) and a MEMS sensor (right), both displayed in m/s. Electromagnetic contamination predominates on the geophone record, but is absent on the MEMS record.

from a recent railway monitoring passive survey. Seismic is indeed the method of choice for monitoring the condition of railway tracks detecting potential sinkholes, and taking preventive measures in good time. On this example, two lines were deployed alongside a railway track, with 10 Hz geophones and MEMS sensors co-located at each receiver position. As expected, the 25,000 V railway power line did not affect the MEMS record, while electromagnetic contamination was predominant on the geophone one.

Spurious frequency

The so-called spurious frequency refers to the resonance of a sensing system perpendicular to its normal (vertical) working axis, and is a combination of multiple modes of movement (Maxwell 1997). It could therefore also be called 'lateral resonant frequency'. Any ground motion in either the transverse or rotational plane may cause the geophone to resonate: the lowest of these resonance modes is called spurious frequency, which specifies the sensor upper frequency limitation.

To further investigate the spurious frequency issue, it is important to remember that the geophone measurement is based on an induced voltage created by the displacement of a mass (i.e., the geophone coil) relatively to a magnet. To enable the proper sensing of the seismic signal, the spring axial stiffness has to be low, to enable both a long stroke (beneficial to sensitivity) and a low natural frequency (that is directly related to the {spring stiffness/proof mass} ratio). The spring's radial stiffness must however be as high as possible, for three reasons: 1) to ensure the rejection of parasitic, non-vertical signal (such as surface and converted waves); 2) to reject parasitic modes (such as resonance modes) that can induce displacements along the sensitive axis; and 3) to ensure insensitivity to tilt (to avoid coil friction against the casing). Despite the efforts made by manufacturers to ensure a low axial stiffness and a high radial one, the rated spurious frequencies remain 'low' and limit the useable geophone bandwidth. Typical values for spurious frequency range from 120-150 Hz for 5 Hz geophones to ~250 Hz for 10 Hz geophones, with a more pronounced effect when the geophone is tilted (the coupling quality having no influence on the spurious phenomenon, despite being a common misconception).

As the MEMS measurement is based on tiny changes in capacitance (through electrodes) induced by microscopic mass displacements, MEMS sensors can be designed with a {spring stiffness/proof mass} ratio that is much higher than that of geophones, which means it is possible to design an oscillating system with a much higher transverse stiffness. Spurious frequencies are therefore well above the useful seismic bandwidth.

In practice, hitting the spurious frequency translates into discontinuities in the geophone transfer function (unexpected phase shift and strong variation in sensitivity), which manifests itself in

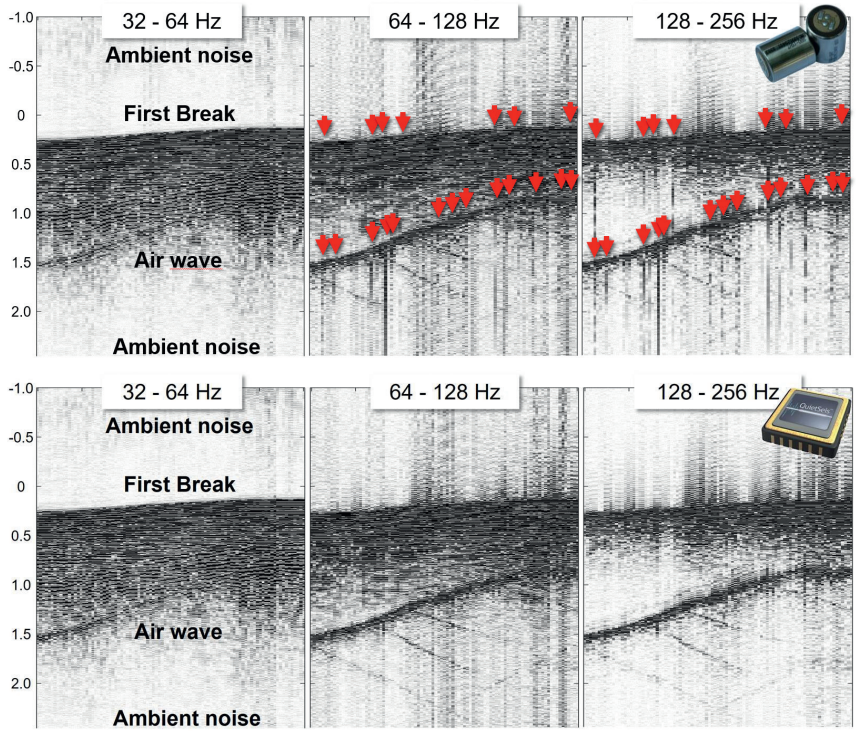

Figure 3 Field data illustration of spurious frequency on field data: 5 Hz geophones (top) and QuietSeis MEMS (bottom). The geophone used for the test is specified with a spurious frequency > 120 Hz.

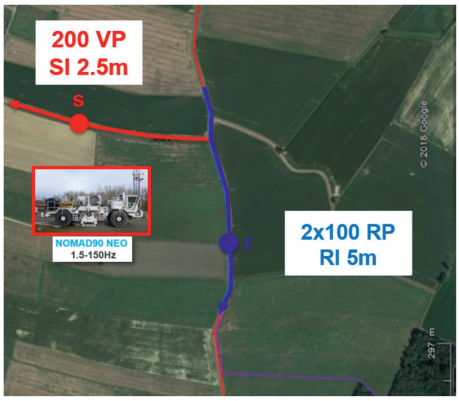

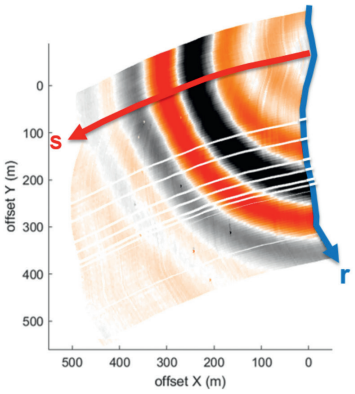

Figure 4 Field test configuration to acquire a portion of cross spread with quasi perpendicular source and receiver lines. Along the source line, 200 source positions spaced 2.5 m apart were shot with a single Nomad 90 Neo vibrator and a broadband 1.5-150 Hz sweep. Along the receiver line, 100 receiver positions spaced 5 m apart involved co-located MEMS (WiNG DFU) sensors and 5 Hz non-Sercel geophones (508XT system). Cross-spread time slices sorted in (offset_X, offset_Y) exhibit circular seismic wave fronts.

seismic data as strong ringing noise running through the record. Figure 3 illustrates this concept of spurious frequencies. On these two 100-channel Common Source Gathers, the highest octaves are contaminated by spurious frequency on numerous geophone channels (red arrows), while the MEMS records remain artefact-free.

Data jitter

Definition

The inherent output signal of a sensor is the result of a convolution of the sensor response with a transient ground motion. Sensor-induced data jitter is an amplitude and phase perturbation induced solely by sensor-to-sensor variations in the sensor response. In theory, this jitter could be corrected with proper deconvolution of the sensor response. This, however, requires good knowledge of the parameters controlling the sensor response. This is not possible for sensors such as geophones, as their parameters (even when brand new) differ from catalogue nominal values (dispersion of individual geophone parameters due to manufacturing tolerances), and will continue to vary throughout the duration of an acquisition project (due to ageing and temperature variations).

The geophone case

A geophone is a mass-spring electromagnetic system with an instrument response defined by three parameters:

- geophone sensitivity $S_g(V/ms^{-1})$;
- corner frequency f_c (Hz);
- damping factor λ.

In the frequency domain, $f\,(Hz)$, the geophone's inherent output $G(f)$ is related to the ground particle velocity $v(f)$ according to:

$$G\left(f\right)=S_g.LC\left(f;\ f_c,\lambda\right).v\left(f\right) \tag{1a}$$

With $f\,(Hz)$ the frequency of the ground particle velocity $v(f)$ and $LC(f;f_c,\lambda)$ a low-cut minimum phase filter defined according to:

$$LC\left(f;\ f_c,\lambda\right)=-f^2/(-f^2+2j\lambda ff_c+f_c^2) \tag{1b}$$

The geophone's parameters $\left(S_g,f_c,\lambda\right)$ are referenced by catalogue values $\left(S_g^c,f_c^c,\lambda^c\right)$ with a percentage of confidence $\left(\pm\Delta S_g^c,\pm\Delta f_c^c,\pm\Delta\lambda^c\right)$. These tolerances are due to:

- Manufacturing tolerances (manufacturer, tilt and sensitivity-dependent);
- Temperature variations (magnetic materials lose magnetism as they heat, but regain magnetism when cooled provided the maximum temperature is below their Curie temperature);
- Ageing (magnets losing their properties, changes in spring stiffness, improper storage, impacts, etc.).

An accurate knowledge of geophone parameters $\left(S_g,f_c,\lambda\right)$ is required to retrieve the ground motion $v(f)$ from the geophone's inherent output $G(f)$. In practice, this deconvolution is performed using the catalogue values $\left(S_g^c,f_c^c,\lambda^c\right)$ not accounting for the actual values:

$$v_g\left(f\right)=G\left(f\right)/\left(S_g^c.LC\left(f;\ f_c^c,\lambda^c\right)\right). \tag{1c}$$

We therefore have an approximate estimate of the ground particle velocity $v_g(f)$:

$$v_g\left(f\right)=v\left(f\right).\left(S_g.LC\left(f;\ f_c,\lambda\right)\right)/\left(S_g^c.LC\left(f;\ f_c^c,\lambda^c\right)\right) \tag{1d}$$

The sensor-to-sensor variations in geophone response not only affect heterogeneous geophone pools available for a given project, but also pools of brand new sensors, and may vary with temperature in the course of the seismic acquisition. The numerous causes of variations in the sensor response make it difficult to recover the true ground motion measured by a geophone sensor.

The MEMS case

MEMS sensors are high-precision silicon-based microelectronic systems with an instrument response defined by a frequency-independent scalar S_m. In the frequency domain, $f\,(Hz)$, the MEMS inherent output $M(f)$ is related to the ground particle acceleration $a(f)$ (i.e., the time derivative of the ground particle velocity $j2\pi f.v\left(f\right)$) according to:

$$M\left(f\right)=S_m.a\left(f\right) \tag{2a}$$

The manufacturing process for MEMS technology is highly accurate with extremely low tolerances in the order of 0.25% for S_m, which is about 10 to 30 times less than the tolerances of geophones. Silicon is a highly stable material which makes the MEMS response insensitive to temperature variations. MEMS is moreover only an extra component on the electronic board and so shows an ageing equivalent to the latter. In addition, for

closed-loop MEMS (that prevent proof mass displacements), the sensor tilt has no impact on S_m.

As a consequence of the above-mentioned characteristics, MEMS are broadband sensors that record all frequencies at the same level, only scaled by the frequency-independent sensor response S_m. The extremely low tolerance on S_m allows for an exact, accurate true phase and nearly true amplitude conversion of the MEMS inherent sensing into ground particle acceleration:

$$a(f) = S_m^{-1}.M(f) \quad (2b)$$

Which can be further transformed into ground particle velocity with an integration:

$$v(f) = (j2\pi f)^{-1}.\ a(f) = (j2\pi f)^{-1}.S_m^{-1}.M(f) \quad (2c)$$

To summarize, MEMS sensors are not affected by data jitter, contrary to geophone sensors.

Field test

To illustrate, assess and compare the level of sensor-related data jitter for different sensor technologies, we designed a specific

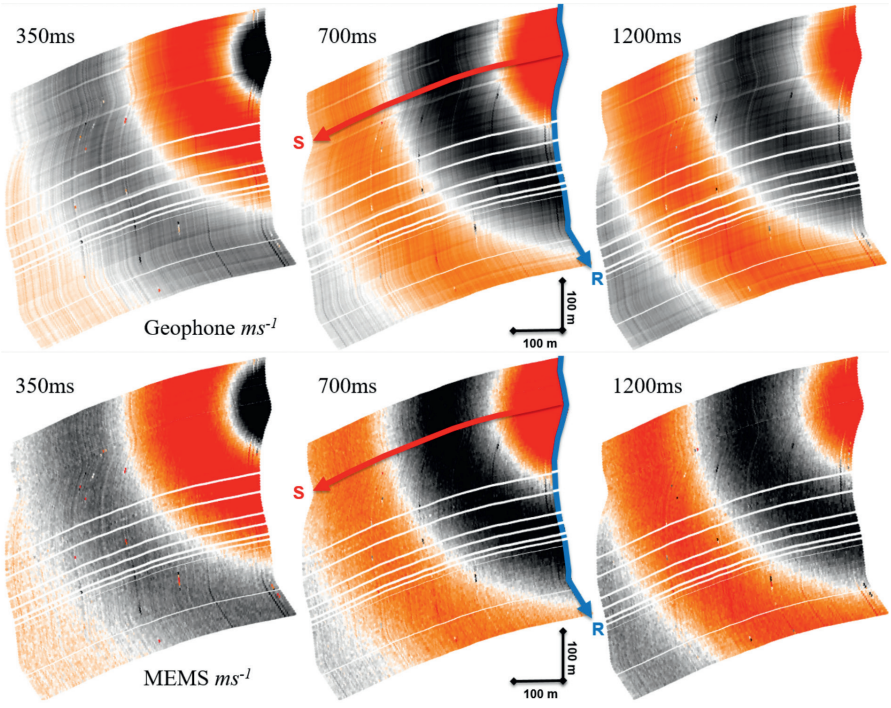

Figure 5a Geophone and MEMS comparison after sensor response correction, [1-2Hz] octave.

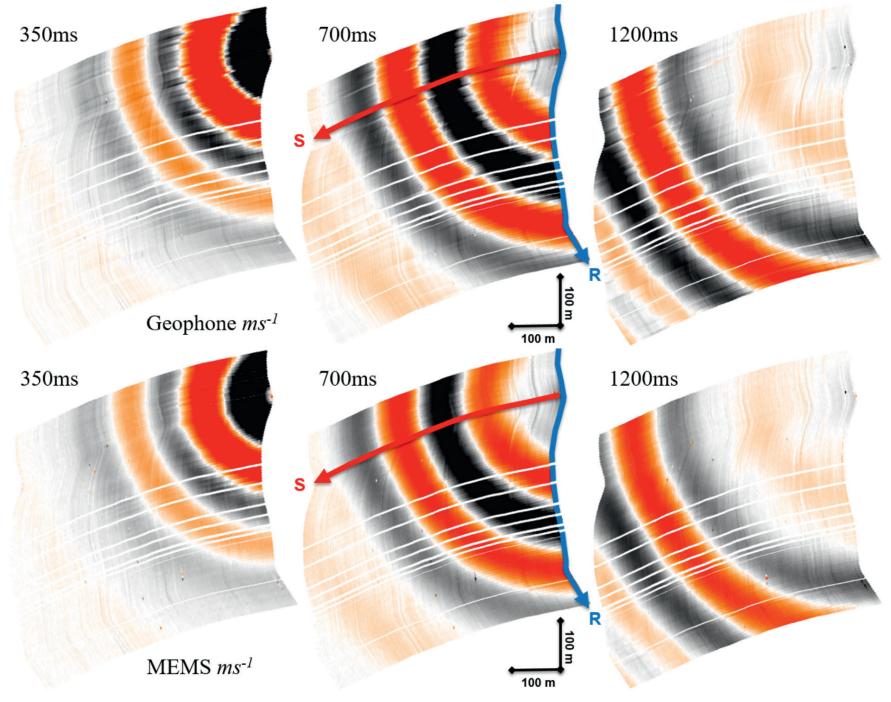

Figure 5b Geophone and MEMS comparison after sensor response correction, [2-4Hz] octave.

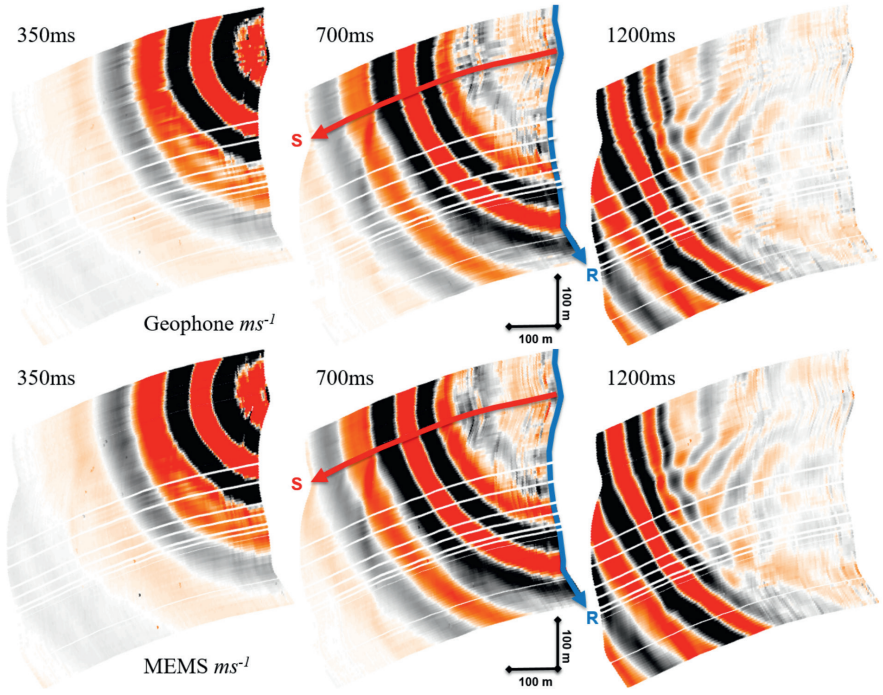

Figure 5c Geophone and MEMS comparison after sensor response correction, [4-8Hz] octave.

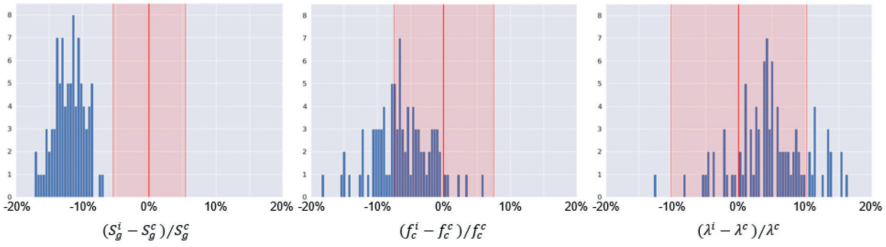

Figure 6 Histogram of the deviation of the 100 inverted geophone closed-circuit parameters $\left(S_g^i, f_c^i, \lambda^i\right)$ from catalogue values $\left(S_g^c, f_c^c, \lambda^c\right)$, expressed as a percentage.

field test consisting of co-located MEMS sensors and high-sensitivity, non-Sercel 5 Hz geophones (Figure 4).

This test makes it possible to measure the impact of a sensor's manufacturing tolerances on seismic data. However, since it was acquired over a small period of time, this test does not make it possible to assess the impact of varying temperature, or the impact of sensor ageing.

Sorting the cross-spread data into in-line and cross-line offsets, the propagating seismic wave fronts are circular while source-to-source variations will manifest themselves with a stripping perpendicular to the source lines and sensor-related data jitter with a stripping perpendicular to the receiver lines. To enable a relevant comparison of geophone and MEMS records, both were corrected for sensor response, as defined in *(1c)* and *(2c)*, for a comparison in the ground particle velocity domain $v\,(ms^{-1})$. Figure 5 compares three time slices at 350 ms, 700 ms and 1200 ms for three octaves. For each of them, seven white lines are visible perpendicular to the receiver lines: they correspond to skipped sensor positions.

The geophone time slices exhibit an octave-dependent data jitter, with sensor-to-sensor phase and amplitude variations. MEMS-related time slices do not exhibit sensor-related data jitter: only a tiny source-to-source stripping can be observed. A closer look also reveals a bulk phase and amplitude shift between the geophone and the MEMS data.

Due to the homogeneity of the seismic signal recorded with MEMS sensors, we used the MEMS data as a reference to invert for geophone parameters $(S_g^i(r), f_c^i(r), \lambda^i(r))_{r=1,..,100}$ which minimize the objective function:

$$min_{\left(S_g^i, f_c^i, \lambda_i\right)} \sum_f \sum_s \left\| w(f).\left(\frac{\boldsymbol{S}_g.LC\left(f;\boldsymbol{f}_c,\lambda\right)}{S_m.(j2\pi f)} - \frac{G(f,s;r)}{M(f,s;r)} \right) \right\| \quad (3)$$

over the range of frequencies f and sources s useable to explain the frequency-dependent amplitude variation and the phase difference between the geophone and MEMS data, $w(f) \sim 1/f$ being a frequency-dependent weighting term. This was done independently for each of the 100 5 Hz geophones. A histogram of the 100 inverted geophone parameters $(S_g^i(r), f_c^i(r), \lambda^i(r))_{r=1,..,100}$, (Figure 6) clearly shows biased distributions, not centered on catalogue values $\left(S_g^c, f_c^c, \lambda^c\right)$ (plain vertical red line) and outside tolerance values $\left(\pm\Delta S_g^c, \pm\Delta f_c^c, \pm\Delta\lambda^c\right)$ (dashed vertical red line). It is the experience of the authors (former crew management & QC's) that low-cost geophones may not respect the specified tolerances (leading to more significant data jitter). The 5 Hz geophone model used for the test is widely used, and rated as intermediate quality.

For each of the 100 deployed geophones, the amplitude ratio *(dB)* can be displayed as well as the phase error *(rad/2π)* between the geophones' inverted and catalogue parameters, as a function of frequency (Figure 7). The plain horizontal red lines represent

geophones with inverted parameters matching catalogue parameters (no error). The dashed red curves represent the maximum deviations allowed by catalogue tolerances $\left(\pm\Delta S_g^c, \pm\Delta f_c^c, \pm\Delta\lambda^c\right)$.

These curves illustrate the following behavior of geophone data jitter:

- A frequency dependency, with an inflection around the geophone corner frequency f_c
- Amplitude and phase errors are:
  - asymptotically constant when $f/f_c << 1$ and $f/f_c >> 1$;
  - outside sensor specifications;
  - biased, not randomly distributed around 0 dB or 0 %.

To check the ability of inverted parameters to correct for data jitter, we can compare the differences in time slices when using catalogue values $\left(S_g^c, f_c^c, \lambda^c\right)$ (Figure 8a) and inverted values $\left(S_g^i, f_c^i, \lambda^i\right)$ (Figure 8b). By doing so, we can observe a significant reduction in the difference between geophone inverted and MEMS time slices over the three octaves displayed.

With MEMS as a reference, we have established how a three-term inversion for factual geophone parameters significantly reduces the difference between geophone and MEMS sensor data. This confirms that the observed differences are mainly due to the deviation of geophone parameters from the catalogue nominal values.

It is the intention of the authors to perform further tests and studies to illustrate the influence of ageing and temperature on data jitter for both sensors, though initial analyses indicates a lower contribution than manufacturing tolerances. This jitter will, however, accumulate with the manufacturing tolerances, yielding more significant uncertainties.

The sensor-induced data jitter is a new concept that has never been illustrated up to now. There are six reasons to explain why:

- The use of geophone arrays mixes the performance of individual geophones;
- When observed, the signal variations from sensor to sensor were attributed to coupling and varying terrain properties;

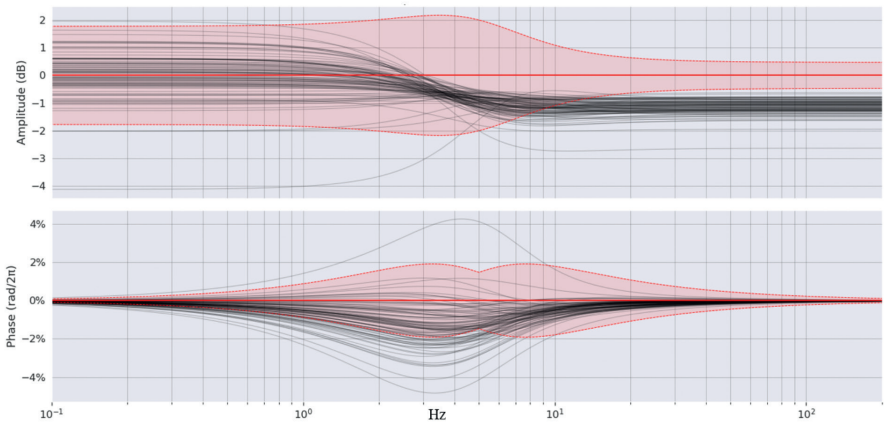

Figure 7 Amplitude and phase error of the geophones: catalogue nominal error (plain red = no error) and error computed with catalogue maximum errors using specified tolerances (dashed red) are compared with the inverted error (black) obtained by field measurement, using the formula $S_g^i.LC\left(f; f_c^i, \lambda^i\right) / S_g^c.LC\left(f; f_c^c, \lambda^c\right)$. It corresponds to the amplitude ratio and phase error between the ground particle velocity derived from geophone using catalogue values and the true ground participle velocity.

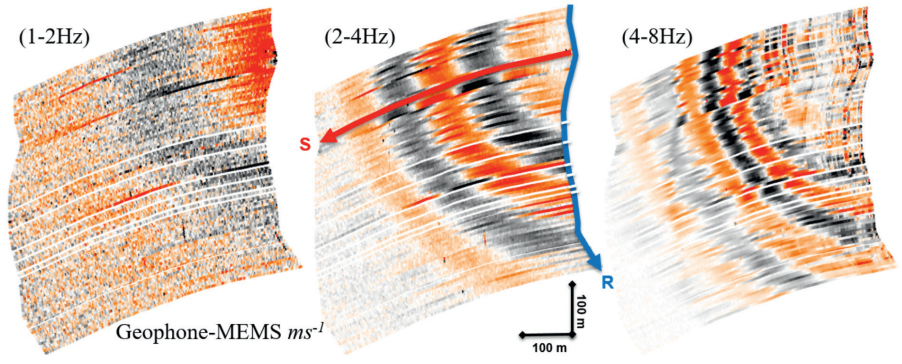

Figure 8a Time slices differences (700 ms) between geophone and MEMS sensors when using catalogue parameters $\left(S_g^c, f_c^c, \lambda^c\right)$ to correct for geophone response.

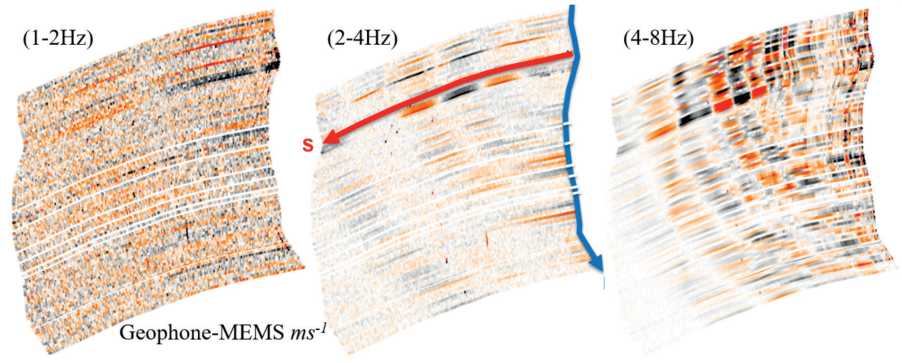

Figure 8b Time slices differences (700 ms) between geophone and MEMS sensors when using inverted parameters $\left(S_g^i, f_c^i, \lambda^i\right)$ to correct for geophone response.

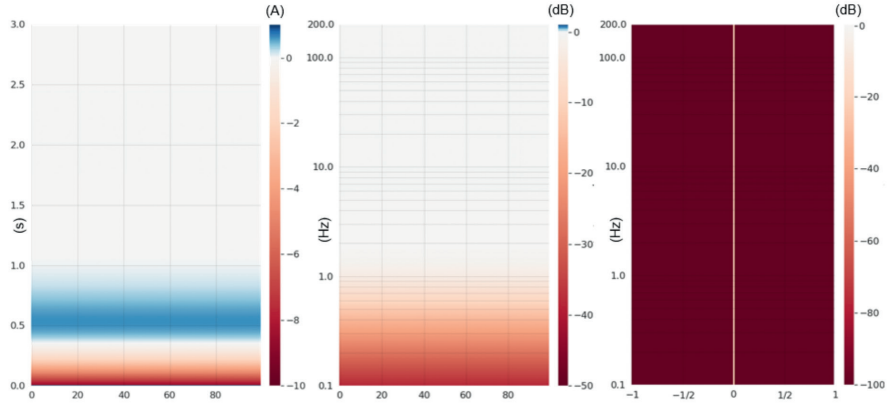

Figure 9a Response of the 100 MEMS sensors (in m/s), corrected for sensor response (equation 2c), to a synthetic horizontal plane wave: time response (left), temporal frequency response (middle), and (right) temporal frequency response (in log scale) versus wave number (normalized by Nyquist).

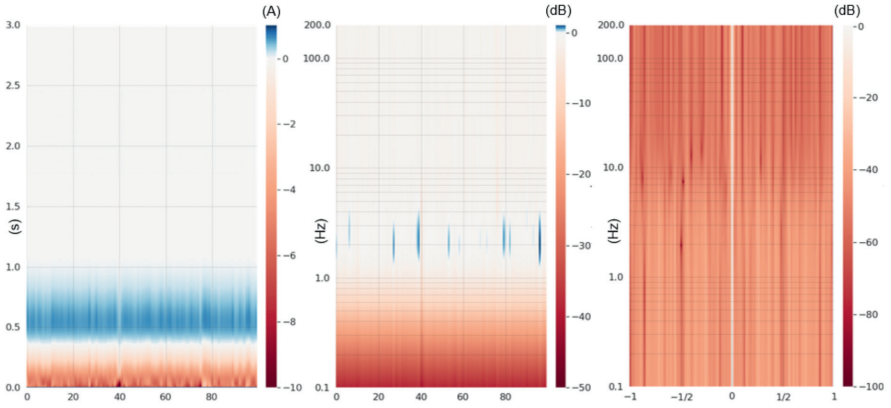

Figure 9b Response of the 100 geophones (in m/s), corrected for sensor response (equation 1d), to a synthetic horizontal plane wave: time response (left), temporal frequency response (middle), and (right) temporal frequency response (in log scale) versus wave number (normalized by Nyquist).

- Low-frequency sources reveal the low-frequency geophone response;
- A finely sampled cross spread eases identification of the data jitter;
- An absence of reference sensors on commercial surveys.
- The jitter observed for geophones concerns not only the geophone, but the whole acquisition chain up to the 'common point' with digital channels (including, for example, the cable connecting the geophone to the digitizer).

Impact of data jitter on seismic imaging

Geophones introduce a data jitter that is directly related to uncertainties in the geophone's characteristic parameters (S, f_c, λ). This introduces a frequency-dependent amplitude and phase distortion in the recorded signal. To correct for these distortions, we would have to know the actual geophone response in the course of the acquisition in order to design a dedicated operator per channel for de-signature. This is barely feasible in practice, even if extra resources are allocated during field operations and at the processing stage. We would in addition need to account for temperature variations when designing the de-signature operator, especially for surveys acquired with significant temperature variations, which is the current case for Arctic or hot desert projects.

The sensor-related jitter has a detrimental impact on signal preservation, starting with the very early stages of processing, when velocity filters are applied for surface-wave removal before any surface-consistent corrections can be derived. Figure 9a represents the temporal (left) and frequency (middle) response of the 100 consecutive MEMS receivers, sensing a synthetic horizontal plane wave with a flat amplitude spectrum beyond 1 Hz. Figure 9a, right, represents its (log(f),k) spectrum with all the energy concentrated around k=0 as a consequence of the lateral invariance of both the plane wave and the MEMS response. This spectral focalization ensures an excellent preservation of the reflection signal after velocity filtering. The situation is quite different with geophones (Figure 9b): the sensor-to-sensor variations introduce a spreading of the signal in the (log(f),k) spectra, with, as a consequence, a damaged signal after application of a velocity filter, especially over low frequencies. This spreading in the (log(f),k) also makes it less effective to remove the surface waves leaking into the signal cone.

One can question the ability of surface-consistent corrections to correct for sensor data jitter. The necessary conditions for success are:

- A signal-to-noise ratio that is high enough for proper phase estimation.
- No multi-channel de-noise across geophones to retrieve individual geophone parameters.
- Introducing an additional three term only $\left(S_g^c, f_c^c, \lambda^c\right)$ parametric form *(equation 1d)* to the receiver operator. Doing so makes it possible to deal with long operators without inversion overfitting.
- No amplitude spectral replacement over low frequencies based on catalogue values for geophone operators

These four conditions are difficult to meet: insufficient surface-consistent correction will then leave a systematic geophone

bias, which will survive the stack whatever the trace density. Contrary to the case with geophones, MEMS sensors have the advantage of not requiring any compensation for sensor-induced data jitter.

Conclusion

On the receiver side, the industry trend is moving towards nodal systems, with single-sensor broadband signal recording. Although project trace densities keep increasing with single-sensor acquisitions, we observe at best a constant but often a decrease in sensor densities actually planted into the ground compared to previous acquisitions. The individual response of each sensor has therefore become as important as our knowledge of the source signature, with a major difference being the fact that the source signature is continuously recorded, contrary to the sensor signatures. In order to exactly transform the recorded data into ground particle motions over a large range of frequencies and avoid sensor-related jitter on the recorded data, it is necessary to operate with sensors having an exactly known and invariant response. As illustrated with a field test, this is the case for MEMS sensors, but not for geophones (even with brand new ones). This data jitter concept has not been identified until now for several reasons (use of arrays that mix individual sensor performance, signal variations from sensor to sensor erroneously attributed to coupling and varying terrain properties, lack of reference sensors on commercial surveys and specific experiments designed to highlight the phenomenon, etc.). Given the exactly known and invariant response of MEMS sensors, they are therefore the sensor of choice to extract the full value from all seismic innovations. With the accuracy and stability of MEMS sensors, it is possible to avoid introducing jitter into the data recorded, resulting in better signal preservation and noise removal. For FWI requirements, MEMS sensors have the inherent capability to record high-fidelity low-frequency signal, and the third generation have also overcome the low-frequency noise-floor limitation of the previous generations: state-of-the-art MEMS sensors therefore enable an exact measurement of broadband ground motions in any units (ms^{-2}, ms^{-1}, m). MEMS is then the perfect sensor to accompany current industry trends. Sercel has every confidence in the benefits of MEMS technology for all seismic applications, from land to OBN through structural monitoring, and sees it as the state-of-the-art seismic sensor best placed to bring unprecedented value to the seismic industry.

Acknowledgments

The authors would like to thank Smart Seismic Solutions (S3) for their support in organizing field tests, Didier Marin (CGG) for his valuable support and expertise in data processing, and numerous Sercel colleagues who contributed to the success of the acquisition test campaign and analysis.

References

Fougerat, A., Guérineau, L. and Tellier, N. [2018] High-quality signal recording down to 0.001 Hz with standard MEMS accelerometers. 88th SEG annual meeting, expanded abstract. DOI: https://doi.org/10.1190/segam2018-2995544.1

Maxwell P. and Faber, K. [1997] Geophone Spurious Frequency – What Is It and How Does It Affect Seismic Data Quality. EAGE 59th Conference & Exhibition, extended abstract. DOI: https://doi.org/10.3997/2214-4609-pdb.131.GEN1997_P046

Lainé, J. and Mougenot, D. [2014] A high-sensitivity MEMS-based accelerometer. *The Leading Edge*, Vol **33** Issue 11, pp. 1210–1308. DOI: https://doi.org/10.1190/tle33111234.1

Shi, S., Du, Y., Yao, Z., Wang, D., Zhang, M., Cheng, S., Gan, L., Gao, L., Li, M. and Qin, Z. [2008] Digital point receiver seismic acquisition and pre-stack reservoir characterization at Sulige gas field, China. 70th EAGE Conference & Exhibition, Expanded Abstract. DOI: https://doi.org/10.3997/2214-4609.20147566

Shi, S., Du, Y., Zhang, M., Cheng, S., Gan, L., Gao, L Yao, Z. and Li, M. [2009] Seismic acquisition with digital point receiver and prestack reservoir characterization at China's Sulige gas field. *The Leading Edge*, **28(**3), 324-331. DOI: https://doi.org/10.1190/1.3104079

Stotter, C. and Angerer, E. [2011] Evaluation of 3C microelectromechanical system data on a 2D line: Direct comparison with conventional vertical-component geophone arrays and PS-wave analysis. *Geophysics* **76**/(3), B79-B87. DOI: https://doi.org/10.1190/1.3561769

Tellier, N. and Lainé, J. [2017] Understanding MEMS-based digital seismic sensors: *First Break*, **35**(1), 93-100. DOI: https://doi.org/0.3997/1365-2397.35.1.87386

Tellier, N., Laroche, S., and Herrmann, Ph. [2020] Native true amplitude and phase broadband sensing now available with the latest MEMS sensors. 90th SEG annual meeting, expanded abstract. DOI: https://doi.org/10.1190/segam2020-3423114.1

Xuming, B., Shenglui, Y., Zedan, W., Jingguo, C., Xiaodong, W. amd Qing, H. [2014] Digital geophones and exploration of tight oil. 84th annual meeting, SEG, expanded abstract. DOI: https://doi.org/10.1190/segam2014-0406.1